Microwave Method for High Frequency Properties of Graphene

Ling Hao, John Gallop

National Physical Laboratory, Teddington, TW11 0LW, UK,

Q. Liu, J. Chen

Department of Mechanical, Aerospace and Civil Engineering, Brunel University Uxbridge, UB8 3PH, UK

Corresponding author: Ling Hao   e-mail: ling.hao@npl.co.uk.

Abstract

Graphene is a remarkable material which is yet to make the transition from unique laboratory phenomenon to useful industrial material. One missing element in the development process is a quick method of quality control of the electrical properties of graphene which may be applied in, or close to, the graphene growth process on an industrial scale. In this paper we describe a non-contact method using microwave resonance which potentially solves this problem. We describe the technique, consider its limitations and accuracy and suggest how the method may have future take up.

1. Introduction

Graphene transport properties have been extensively studied ever since the discovery of this unique single atomic thickness material in 2004. The high mobility values obtained at room temperature combined with the other significant electronic properties such as massless carriers, gapless conductivity in the ideal case, combined with induced energy gaps from gating electric fields and carrier concentration adjustment by adsorbate doping [1-6].   Each advantage arising from these unusual properties generally also brings complications. So for example it is problematic to produce low resistance electrical contacts to graphene samples because of the extremely thin films which are readily damaged but also because the proximity of a different conducting layer will dope the carrier concentration and alter the mobility of the graphene in the neighbourhood of the contact. Many other effects like this complicate the important requirement of the measurement of transport properties of graphene. In this paper we outline a novel measurement method which allows us to avoid most of the complications mentioned above.

The essence of the technique relies on several factors. First, although graphene has a high 3D conductivity (less than some metals but much higher than typical semiconductors), the 2D sheet resistance of graphene is comparable with the impedance of free space $(\mu_0/\varepsilon_0)^{1/2}$. Second, a monolayer or even a few-layer thick sample of graphene does not have a significant attenuation effect on electric fields which are parallel to its surface. Third, as a diamagnet, its relative permeability can be assumed to be close to unity.

These factors, when taken together, suggest that a non-contacting method of measuring the conductivity may be applicable. We have developed a microwave resonance technique, based on the perturbation of a high Q dielectric resonator by the presence of a nearby sample of graphene [7]. We have shown that it is possible to convert this technique by a method of substitution, into an accurate and fast method for deriving sheet resistance (or equivalently, 2D conductivity) without the need for patterning or making contacts.

2. Microwave cavity perturbation method

A vector network analyser (VNA- Hewlett Packard 8720) is used to measure the S-parameters of a two-port resonator, at any frequency between 2 and 20 GHz. Using the bandwidth measurement function this instrument enables the centre frequency, insertion loss and linewidth of any of the resonances of the system to be measured. In addition, to improve the measurement accuracy, we have written a Labview virtual instrument program allowing the same parameters to be determined via a non-linear least-squares fitting routine to a skewed Lorentzian lineshape. Using the latter software provides a measurement of these parameters with typically ten times lower uncertainty than achieved by repeated measurements using the internal instrument evaluation routine.

We make use of the system shown schematically in Figure 1(a). A sapphire (single crystal Al_2O_3) cylindrical 'puck' (12.5 mm in diameter and 5 mm in height) is situated in the centre of a cylindrical copper housing, 20mm inner diameter and 20mm high. The puck is supported by a 5mm high quartz tube spacer. The sapphire single crystal is cut with its c-axis parallel to the axis of the cylinder. The sapphire has relative permittivities of 11.6 (c-axis) and 9.4 (a-b plane) with a loss tangent of $< 10^{-5}$.
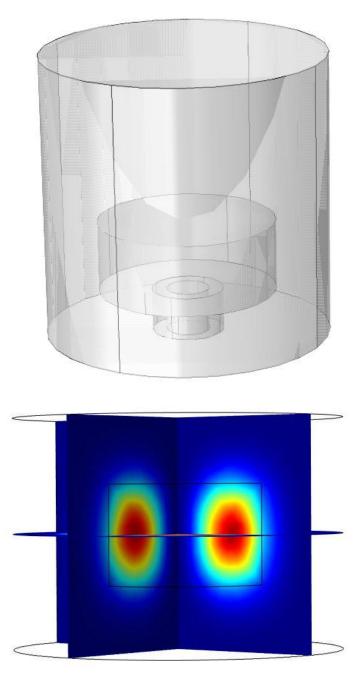

Figure 1: a) The Sapphire puck system with quartz supporting ring inside a Cu housing. b) Finite element modelling result shows transverse electric fields density for TE010 mode in the single crystal Al_2O_3 puck. The copper housing contains two SMA connectors with attached antennae protruding slightly into the housing, made from short wire probes connected to the centre conductor and bent through 90° in the horizontal plane. This arrangement is designed to couple to transverse electric fields.

Measuring the transmission S_{21} parameter between 8 GHz and 20 GHz the combined housing and dielectric puck demonstrates a number of sharp resonance peaks. These represent modes in which there are low-loss standing waves, some of which are predominantly in the sapphire region, some mainly within the

empty volume of the copper housing while a third type has a mixed standing wave pattern in both regions. It is possible to distinguish these by the observed resonance linewidths (or equivalently the Q value). Modes in which most of the field is confined within the sapphire have higher Q values (typically around 10^4) whereas the other modes have lower Qs, in the region of 10^3, on account of additional ohmic losses on the copper surfaces. The lowest frequency sapphire dielectric resonator mode is the TE010 mode. A colour plot of the transverse electric field density is shown in Fig. 1b), calculated from COMSOL finite element software. Note the high degree of confinement but also that there is a finite TE field strength in the region above the sapphire.

Now the essential feature of our method is that a graphene sample may be brought into this near-field region. Typically the graphene layer will be on an insulating substrate with low microwave loss. It is generally necessary to provide a fixed spacer between graphene sample and sapphire puck and this is done by placing a 3mm high quartz tube spacer on the puck with the graphene substrate situated on-top of this spacer. The remarkable result of including a graphene sample in this situation is that, provided the graphene is of reasonably high quality without too high a concentration of defects, the impact on the Q factor is dramatic, typically being reduced from 10^4 to only a few hundred (see Fig. 2).

This is particularly surprising given that the volume of graphene material involved is only around $10^{-14}m^3$ or more than 10^7 less than the volume of the puck resonator. So the graphene causes a very dramatic change in the losses in the system. Of course this observation does not ensure that the observed change can be converted into a measurement of graphene properties. To bring about this calculation several further stages must be considered. A point to note is that the large change in Q value is caused by ohmic losses in the graphene film arising from electric currents flowing in phase with the driving microwave electric fields. In order to drive these currents it is only electric field components in the x-y plane which can do this. For this reason we limit our consideration to purely TE modes in this study. Only TE modes are capable of satisfying the requirements of our simple substitutional measurement method for deriving the graphene electrical conductivity, as will be described in the next section.

In principle if the position of the graphene sample was accurately known a finite element model could be used to calculate the linewidth shift arising from the presence of a graphene sample of known sheet resistance [8-11]. In reality this is very problematic. First the difficulty of accurately meshing the finite element model to give suitably high spatial resolution that the model deals accurately with layers of only 10^{-10} m thickness as well as structures of 20mm in size means that accurate 3D modelling cannot be realistically achieved in a short time. Instead we resort to a substitution method to convert the large observed *Q* change into an accurate value for graphene conductivity. First, notice that the skin depth at microwave frequencies in graphene is far greater than the thickness of few layer graphene. A typical value for 3D resistivity of graphene is around 3 μΩm so at a frequency of around 10 GHz the skin depth δ is given by

$$\delta = \left(\frac{2\rho}{\omega\mu_r\mu_0}\right)^{\frac{1}{2}} \sim 10\mu m \qquad\qquad .....(1)$$

Note that this is some 10^4 times the thickness of the graphene itself. Thus the graphene film will not screen the electromagnetic fields from the underlying substrate to a detectable extent. This result indicates the next step in the substitution method. If now another measurement of the Q value is made in which a bare substrate of the same material, size and thickness as the one containing graphene is substituted into the housing, in the same position, we can measure the new values of the Q and resonant frequency.

3. *Modelling of resonator perturbation*

From the discussion of the previous section we may assume, to a good approximation, that the field distributions in the bare substrate and graphene coated substrate situations are the same. In this situation perturbation theory may be reliably applied to evaluate the surface impedance of the graphene, provided

only that the complex permittivity and the thickness of the bare substrate are known. We limit ourselves to first order perturbation theory at this stage. Consider that the substrate complex permittivity is $\varepsilon_s' + i\varepsilon_s''$ whereas the permittivity of graphene is $\varepsilon_g' + i\varepsilon_g''$. We can calculate the frequency shift Δf_s produced in a certain resonance by the presence of the bare substrate from the following equation

$$\Delta f_s = f_0\left(\frac{(\varepsilon_s'-1)\int E^2 dV}{W}\right) \quad\quad .....(2)$$

where W is the total stored energy in the microwave fields within the housing, E is the electric field and the integral is over the volume V of the substrate, f_0 is the unperturbed resonant frequency of the empty housing. We can similarly use perturbation theory to calculate Δw_s the shift in the linewidth of the same mode:-

$$\Delta w_s = 2f_0\left(\frac{\varepsilon_s''\int E^2 dV}{W}\right) \quad\quad .....(3)$$

With the graphene covered substrate in place similar expressions can be written for frequency and linewidth shifts

$$\Delta f_g = f_0\left(\frac{(\varepsilon_s'-1)\int E^2 dV+(\varepsilon_g'-1)\int E^2 dv}{W}\right) \quad\quad .....(4)$$

$$\Delta w_g = 2f_0\left(\frac{\varepsilon_s''\int E^2 dV+\varepsilon_g''\int E^2 dv}{W}\right) \quad\quad .....(5)$$

where now, as well as integrals over the substrate volume V we also take integrals over the graphene layer volume v.

As we have already shown that the graphene film is far too thin to screen the electric field from its underlying substrate the electric field spatial distribution within the housing and dielectric resonator is the same in the situation with bare substrate and with graphene coated substrate. This assumption allows us to simplify the above four equations to yield a relationship between the easily measurable quantities Δf_s and $(\Delta w_g - \Delta w_s)$

$$\Delta w_g - \Delta w_s = 2f_0\left(\frac{\varepsilon_g''\int E^2 dv}{W}\right)=\varepsilon_g''\frac{2\Delta f_s t_g}{(\varepsilon_s'-1)\,t_s} \quad\quad .....(6)$$

The only unknowns remaining in this equation are ε_g'' and t_g. Note there is a simple relationship between the 3D conductivity of a material σ and the imaginary component of its permittivity and this allows us to rewrite equation (5) in terms of σ:

$$\sigma = 2\pi\, f_0\varepsilon_0\varepsilon_g'' = \frac{\pi\, f_0\varepsilon_0\left(\Delta w_g-\Delta w_s\right)\left(\varepsilon_s'-1\right)t_s}{\Delta f_s t_g} \quad\quad .....(7)$$

The 3D conductivity still requires a knowledge of t_g but for 2D materials like graphene it is really the 2D transport properties which are important. Thus we can convert the 3D conductivity to 2D sheet resistance R_s using the relationship $\sigma = t_g/R_s$

$$R_s = \frac{\Delta f_s}{\pi\, f_0\varepsilon_0\left(\Delta w_g-\Delta w_s\right)\left(\varepsilon_s'-1\right)t_s} \quad\quad .....(8)$$

Thus a simple three stage measurement of a chosen high Q transverse electric microwave resonance

4. Results and Discussion

Graphene is expected to have a wide range of important applications ranging from high frequency FETs for post Moore's Law electronics, through chemical and physical nanosensors to corrosion resistant coatings and improved performance of composites, to name just a few. Synthesis of graphene products with the appropriate properties for these specific applications is based on a variety of different growth methods which give rise to a wide range of electrical properties. These include chemical vapour deposition (CVD ([12-13], high temperature decomposition of SiC [14-17] and reduction of graphene oxide [18-19]. But whatever growth method (exfoliation of graphite, chemical vapour deposition, epitaxial decomposition or chemical synthesis from hydrocarbons) there is a need for quality control of these processes based on measuring the electronic properties. The 2D conductivity values typically achieved by these various growth techniques vary across more than four orders of magnitude. We have measured graphene samples synthesized by many of these different methods. For each graphene sample measurement a set of the three frequency dependent transmission traces have been recorded, as shown in Figure 2. First the TE010 resonance of the sapphire puck trace is measured using the VNA and the resulting trace is fitted to a skewed Lorentzian lineshape. Next a bare substrate is placed close to the puck, causing the resonance frequency to shift down but the Q value is essentially unchanged since the substrate material is chosen to have a low loss tangent. Finally graphene on an identical substrate shows a much reduced Q value though the frequency is not detectably shifted from that of the bare substrate since the *sheet reactance* of the graphene is negligible.

Table 1 shows a series of results for a variety of graphene samples grown by different methods including SiC epitaxial growth, chemical vapour deposition and graphene oxide reduction. One issue of note is the wide variation in sheet resistance values which these samples exhibit and which substitutional technique is capable of measuring. In cases of high sheet resistance the sample should be brought closer to the sapphire surface, in order to increase the influence on linewidth of the resonance. We have developed a small nylon clamp which is mounted on a nylon screw, inserted in the lid of the resonator, allowing the vertical position of the substrate to be adjusted to optimise the measurements. The results summarised in the Table indicate that the sheet resistance varies by three orders of magnitude between the best quality epitaxial graphene on SiC and the reduced graphene oxide sample. In fact the basic method is capable of an even greater range of sheet resistance measurements. We believe that values in the range from 10 Ω to 1 MΩ can be accurately measured although we have not yet received samples at the extremes of this range. In addition we have shown that the microwave measurements agree well with conventional contacting low frequency sheet resistance measurements using a four terminal van der Pauw method. Agreement is at the level of 10% but this is to be contrasted with the microwave method for which the reproducibility from measurement to measurement is better than 1%.

Note that for CVD growth the sheet resistance varies quite widely between samples, depending on the growth process and transfer process. Figure 3 shows an AFM topography image of the CVD sample with a low value of sheet resistance, where we can see wrinkles in the graphene surface showing that it follows the polishing striations of the growth substrate (copper in this case) and forms some additional wrinkles on transfer to a quartz substrate. There is a little surface contamination on this sample in the form of residual polymer from the transfer stage.
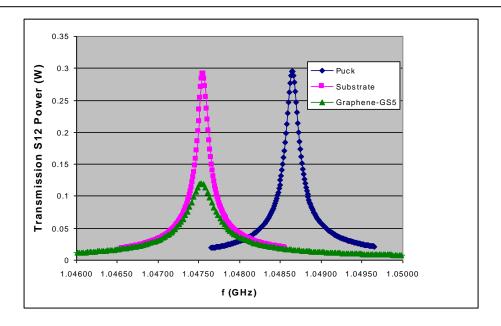
Fig. 2 Plot of the Lorentzian lineshape of the TE010 resonance of the sapphire puck shows a set of VNA traces for the three stages of the measurement process. Curve A (blue –puck) shows the high Q Lorentzian lineshape observed for the resonator with no substrate. Note that the linewidth is around 1 MHz. The second curve (B in pink) is shifted down in frequency by the presence of a bare quartz substrate but the Q value is essentially unchanged since the quartz substrate has a very low loss tangent. The third curve (C) with an identical quartz substrate coated with CVD graphene shows a much reduced Q value though the frequency is only slightly shifted from that of the bare substrate.

Table 1. Summary of graphene sheet resistance results.

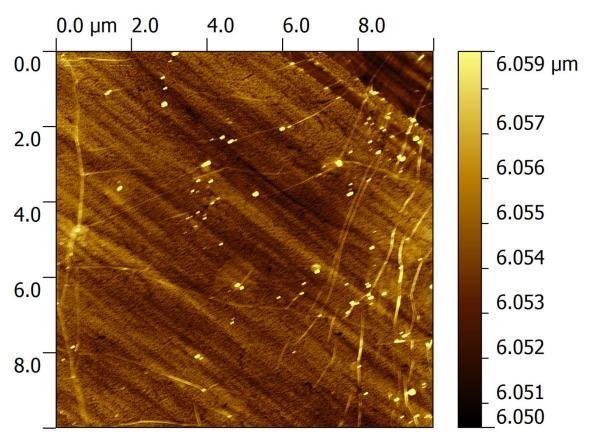| Sample	Graphene thickness (nm)	f_0 (GHz)	Δf (MHz)	$\Delta w_g - \Delta w_s$ (MHz)	3D conductivity σ (S/m)	Sheet resistance R_s ($\Omega/\square$)
1-layer reduced GO	0.4	10.550	1.169	0.0243	4.82×10^4	96400
1-layer CVD	0.4	10.459	140.7	10.91	1.92×10^5	6067
1-layer CVD	0.4	10.4596	76.86	19.35	4.63×10^4	540
1-layer SiC (266)	0.4	10.561	140.7	47.30	2.03×10^7	123.4
1-layer SiC (489)	0.352	10.4816	1.046	3.74	8.57×10^6	318.2

Fig. 3 AFM image of a CVD graphene sample grown on copper and then transferred to a quartz substrate.

4.1. Limitations of the method

The above first order perturbation theory has of course limitations. The four equations above (1-4) assume that the electric field is uniform throughout the substrate thickness. This is a reasonable assumption provided the substrate thickness is much less than the distance between the puck upper surface and the substrate and provided the permittivity of the substrate is not too large. If these conditions are not readily satisfied there is a straightforward check on these assumptions. The measurement can be repeated with the graphene layer uppermost on the substrate. If the sheet resistance appears different it is probable that one or other of the above assumptions is not satisfied. Taking the mean of the two measurements should never the less provide a reasonable approximation to the real value.

A second issue concerns the averaging process over the substrate. It is clear that the method produces an average value of sheet resistance over the area of the graphene coating, weighted according to the transverse electric field intensity at the graphene surface. For the example of the TE010 mode used above the TE mode goes to zero on the axis. Thus the method gives very low weight to the material situated close to the axis. This weighting can be allowed for by displacing the sample from the axis or rotating it in the case of a non-rotationally symmetric mode.

4.2. Modifications of the Method to Measure Two-sided Samples

Some graphene growth methods result in graphene layers being grown on both sides of a substrate (e.g. epitaxial decomposition of the surface of SiC single crystal). The C face grows a rather thicker graphene layer whereas the Si face produces the best quality films. In this case our method described above would provide a measurement of the sum of the sheet resistances added in parallel. It would be useful in such instances to be able to measure the contribution of each layer separately. By using a highly reflecting surface against which the substrate is clamped we have developed a method to do this (see Fig. 4).
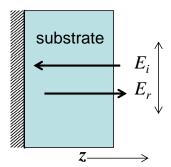
Cu surface

Fig. 4 Schematic of incident and reflected waves from a highly conductive sheet of copper behind the two-sided graphene coated substrate.

Consider the wave equation for a plane electromagnetic wave travelling in the z direction towards a perfectly conducting x-y plane at $z = 0$. The electric field is polarised along the x-axis so we can write for this component:

$$E_x = E_0 e^{(j\omega t - \beta z)} e^{-\alpha z} \qquad .....(8)$$

Maxwell's equations for a conductor of conductivity σ reduce to the following modified wave equation:

$$\nabla^2 E = \mu_0 \, \epsilon_r \epsilon_0 \frac{\partial^2 E}{\partial t^2} + \mu_0 \sigma \frac{\partial E}{\partial t} \qquad ......(9)$$

Now substitute the plane wave solution into equation (9), equating real and imaginary parts to solve for the propagation constant α and β. For a good conductor such that

$$\sigma \gg \epsilon_r \epsilon_0 \omega$$

these reduce to:-

$$\alpha_c = \beta_c = \sqrt{\frac{\mu_0 \sigma \omega}{2}}$$

Now consider both the incident and reflected waves

$$E_i = E_{i0} e^{(j\omega t - \beta z)}$$
$$E_r = E_{r0} e^{(j\omega t + \beta z)}$$

Applying the boundary conditions for continuity of the tangential E and H fields at the conducting surface:

$$\frac{E_{r0}}{E_{i0}} = \frac{\left((1-j)\sqrt{\frac{\mu_0 \sigma \omega}{2}} - 1 \right)}{\left((1-j)\sqrt{\frac{\mu_0 \sigma \omega}{2}} + 1 \right)} \qquad .....(10)$$

If we first assume that the boundary is perfectly conducting the boundary conditions above reduce to

$$\frac{E_{r0}}{E_{i0}} = -1 \qquad .....(11)$$

so that the incident and reflected wave are π out of phase (cancelling exactly at the perfect conductor reflection surface). To calculate the field at some point a distance z from the prefect reflector we merely have to add the incident and reflected waves at this point, remembering that the incoming wave propagates as $e^{(j\omega t - \beta z)}$ whereas the reflected wave propagates as $e^{(j\omega t + \beta z)}$. Thus the amplitude of the electric field at z becomes

$$E_{tot}(z) = E_i(z) + E_r(z)$$
$$E_{tot} = E_i\left(e^{j\beta z} - e^{-j\beta z}\right) = 2E_i I \sinh(\beta z) \qquad .....(12)$$

To understand the influence of the shorting plane on the puck measurements it is necessary to recalculate the expression for the frequency shift Δf_s observed in the puck system when the empty housing is replaced by a bare dielectric substrate. Here is the expression, where now the integral is over the thickness of the substrate, from the conducting plane to the surface furthest from this which contains the graphene. (Note that there will be no contribution to the puck loss from the graphene film next to the conducting plane, in principle).

$$\Delta f_s = f_0 \left(\frac{(\varepsilon_s' - 1) \int_0^{t_s} E_{tot}(z)^2 \, dz}{W} \right) \qquad .....(13)$$

where $E_{tot}(z)$ is the field within the substrate (for now assumed uniform in the x-y plane) and the integral is over the substrate volume. W is the total stored energy in the puck and substrate system. ε_s' is real part of the substrate permittivity.

The other readily measurable quantity is the change in linewidth (Δw_g-Δw_s) and this is unchanged and is expressed as

$$\Delta w_g - \Delta w_s = f_0 \left(\frac{\varepsilon_g'' \int_z^{z+t_g} E_{tot}(z)^2 \, dz}{W} \right) \approx \varepsilon_g'' \frac{3\Delta f_s t_g}{(\varepsilon_s' - 1) t_s} \qquad .....(14)$$

Here we have assumed that for the graphene film the electric field is uniform throughout its thickness, a reasonable assumption provided the substrate is much thinner than the height of the puck. The electric field is not constant throughout the thickness of the substrate, due to the presence of the conducting plane. Provided that t_s << λ/2 where λ is the free space wavelength in the substrate the electric field varies linearly with z, from 0 at the conducting plane, to $E_{tot}(t_g)$ at the graphene surface. The effect of this linear variation on the value of the integral in equation (4) is to reduce its value by 3, compared with the blank substrate with no conducting plane. So finally our expression for R_s becomes independent of graphene thickness t_g

$$R_s = \frac{3\Delta f_s}{2\pi \, f_0 \varepsilon_0 \left(\Delta w_g - \Delta w_s \right) \left(\varepsilon_s' - 1 \right) t_s} \qquad ....(15)$$

Note that the expression for R_s is similar to that of equation (7) above, except that the numerical scaling factor is different. However there is actually a more significant difference. The presence of the highly conducting shorting plane actually significantly reduces the value of the observed changes in frequency and Q so although we now have a method for separately measuring the properties of two sided epitaxial graphene substrates the method is somewhat less sensitive than for a one sided graphene sample.

4.3. Open Resonator Modification

The method as so far described allows fast non-contact measurement of graphene conductivity, with a sensing area of around 100mm^2. Making use of Labview software which we have developed to run the VNA measurement the entire three stage substitution measurement can be carried out in under one minute. However to be applicable to an industrial graphene growth environment, where sheets up to metres in width and length may be involved it is necessary to consider further development. On major potential application of large scale graphene is for touch screens, to replace the need for expensive, scarce and environmentally destructive indium. The first issue is that it is not necessary to use a closed housing for the dielectric resonator. By sacrificing the highest Q values it is possible to operate the resonator system as shown in Fig. 1a with the top of the housing removed. The housing should be reduced in height and the graphene coated substrate is placed over the top so that the film is in a fixed position relative to the fringing field above the sapphire puck. Linewidth measurements of the dielectric resonance may be made in a time scale of less than 1 second so in principle quality control measurements may be made in real time as the graphene coated substrate is passed. The frequency shift, if any, would indicate changes in thickness or permittivity of the substrate.

5. Future Applications

At present the measurement system we have described here makes use of an expensive vector network analyser. We have also built a much simpler and cheaper system based on the concept of the loop oscillator. A microwave amplifier connects the output port of the resonator system to the input port, via a fixed bandwidth filter, centred on the mode frequency, a variable attenuator, a fast microwave switch and an adjustable phase shifter (see Fig. 5).
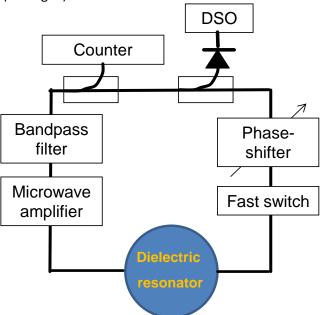

Fig. 5 Schematic layout of loop oscillator based system for graphene non-contacting conductivity measurement.

Each of these is a simple cheap component. By adjusting the phase shifter the amplified signal returned to the input can be arranged to be in-phase with the oscillation within the cavity. Under this condition thermal noise at the resonant frequency will be amplified until the resonator system begins to self-oscillate at the resonant frequency. This frequency can be measured directly with a counter. On opening the microwave switch the output power from the resonator system dies away at a rate set by the linewidth of the resonance and this may be measured directly. Thus the frequency shift and linewidth changes brought about by the substitutions described above can be simply measured without requiring the full capabilities of a vector network analyser.

In the prototype system we have used single crystal sapphire dielectric resonator. When we build a system to look at larger area samples such as will be encountered in an on-line industrial process- control

environment the cost of larger single crystal sapphire resonators will become significant. Fortunately it will be possible to make use of cheaper dielectrics such as alumina which will not seriously compromise performance but will be significantly cheaper. We have also begun to model dielectric resonator geometries which will better match the industrial production requirements. For example a rectangular parallelepiped resonator supports transverse electric field resonant modes which will produce a very uniform average over a rectangular-shaped area, allowing material on a production line to moves past the resonator with accurate sensing of all parts of the production line.

6. Conclusions

Graphene has brought to physics and materials science a wide range of unexpected and fascinating new properties. Much speculation has taken place about its potential applications, ranging from the material to take over from silicon to continue the Moore's Law trajectory, to the idea of using it in space elevators. For the electronics field these are most likely in the areas of flexible electronics (including touch screens) [19-20] and high frequency devices [21-24]. Many barriers must be overcome before the material can find genuine industrial and commercial uses. In this paper we have outlined how at least one such barrier can be overcome, to allow fast, straightforward non-invasive measurements of its electrical properties to be made. We hope that this will assist in a small way towards the real-world applications of this one-atom thick wonder material.

7. Acknowledgments

References
[1]. Novoselov, K. S., Geim, A.K., Morozov, S. V., Jian, D.,   'Electric Field Effect in Atomically Thin Carbon Films', Science, 2004, 306, pp.666-9
[2]. Yuanbo, Z., Yan-Wen, T., Stormer, H.,L., et al., 'Experimental Observation of Quantum Hall Effect and Berry's Phase in Graphene', Nature, 2005, 438 pp.201-4
[3]. Geim A. K., Novoselov K. S., 'The rise of graphene', Nature Materials, 2007, 6 pp. 183-92
[4]. Castro Neto, A. H., Guinea, F., Peres, N. M. R., et al., 'The electronic properties of graphene', Rev. Mod. Phys., 2009, 81 pp.109-62
[5]. Geim. A.K., and Novoselov. K. S., 'Graphene: status and prospects', Science, 2009, 324 pp. 1530-5
[6]. Novoselov. K. S., Fal' ko. V. I., Colombo, L., et al., 'A roadmap for graphene', Nature, 2012, 490 pp. 192–200
[7]. Hao. L., Gallop. J., Goniszewski. S., et al., 'Non-contact method for measurement of the microwave conductivity of graphene' Appl. Phys. Lett., 2013, 103, 123103
[8]. Krupka . J. and Strupinski. W., 'Measurements of the sheet resistance and conductivity of thin epitaxial graphene and SiC films', Appl. Phys. Lett., 2010, 96, 082101
 [9]. Hao. L., Mattevi. C., Gallop. J., et al., 'Microwave surface impedance measurements on reduced graphene oxide', Nanotechnology, 2012, 23, 285706
[10]. Shaforost, O. , Wang, K. , Adabi, M. , et al., 'Microwave characterization of large area graphene using a TE01δ dielectric resonator' IEEE Kharkiv Conference Proceedings 2013.
[11] Gregory, A., Hao, L., Klein, et al., 'Spatially Resolved Electrical Characterisation of Graphene Layers by an Evanescent Field Microwave Microscope', Physica E-Low-Dimensional Systems & Nanostructures 2014, 56, 431.
[12] Li, X. S., Weiwei, C., Jinho, A., et al. 'Large-area synthesis of high-quality and uniform graphene films on copper foils', Science, 2009, 324, 1312–1314

[13] Bae, S., Hyeongkeun, K., Youngbin, L., et al. 'Roll-to-roll production of 30-inch graphene films for transparent Electrodes' Nature Nanotechnol, 2010, 5, 574–578

[14] Emtsev, K. V., Speck, F., Sayller. Th., et al, "Interaction, Growth, and Ordering of Epitaxial Graphene on Sic{0001} Surfaces: A Comparative Photoelectron Spectroscopy Study," Phys. Rev. B, 2008, 77, 155303

[15] Yakimova, R., Virojanadara, C., Gogova, D., et al, "Analysis of the Formation Conditions for Large Area Epitaxial Graphene on Si C Substrates," Mater. Sci. Forum, 2010, 645-648, 565-568

[16]. Eriksson. J., Pearce, R., Iakimov, T., et al, "The Influence of Substrate Morphology on Thickness Uniformity and Unintentional Doping of Epitaxial Graphene on SiC," Appl. Phys. Lett., 2012, 100, 241607

[17] Kopylov, S., Tzalenchuk, A., Kubatkin, S., and Fal'ko, V.I., "Charge Transfer between Epitaxial Graphene and Silicon Carbide". Appl. Phys. Lett., 2010, 97, 112109-112103

[18] Coleman, J. N. et al. Two-dimensional nanosheets produced by liquid exfoliation of layered materials. Science 2011, 331, 568–571

[19] Hernandez, Y., Mutaffa, L., O'Neill, A., et al. High-yield production of graphene by liquid-phase exfoliation of graphite. Nature Nanotechnol., 2003, 3, 563–568

[20] Han, T. H,. Youngbin, L., Choi, M., et al. 'Extremely efficient flexible organic light-emitting diodes with modified graphene anode.' Nature Photon., 2012, 6, 105–110

[21] Liao, L., Jingwei, B., Cheung, R., et al. Sub-100 nm channel length graphene transistors. Nano Lett. 2010, 10, 3952–3956

[22] Han, S. J., Jenkins, K, A., Garcia, A.V., et al. 'High-frequency graphene voltage amplifier.' Nano Lett., 2011, 11, 3690–3693

[23] Kim, K., Choi, J. Y., Kim, T., Cho, S. H. & Chung, H. J.' A role for graphene in silicon based semiconductor devices.' Nature, 2011, 479, 338–344

[24] Britnell, L., Gorbachez, R.V., Jalil, R., et al. 'Field-effect tunneling transistor based on vertical graphene heterostructures.' Science, 2012, 335, 947–950